White Light-Emitting Diodes With Enhanced Efficiency and Thermal Stability Optimized by Quantum Dots-Silica Nanoparticles

Bin Xie, Yanhua Cheng, Junjie Hao, Xingjian Yu, Weicheng Shu, Kai Wang, *Member, IEEE*, and Xiaobing Luo, *Fellow, IEEE*

***Abstract*— White light-emitting diodes (WLEDs) composed of blue LED chip, yellow phosphor, and red quantum dots (QDs) are considered as a potential alternative for the next-generation artificial light source, with their high luminous efficiency (LE) and color-rendering index (CRI). However, the poor stability of QDs-silicone mixture and the optical reabsorption effect between the mixed QDs/phosphor particles severely hinders the wide utilization of QDs-WLEDs. Therefore, in this paper, a silica shell was coated onto the QDs surface to solve the compatibility problem between QDs and phosphor-silicone gel. Then, a QDs-on-chip packaging structure was proposed to reduce the reabsorption energy loss. The prepared QDs@silica nanoparticles (QSNs) exhibited excellent luminescent stability over bare QDs under high-temperature (85 °C) and high-relative humidity (85% RH). With CRI > 90 and R9 > 90, the newly proposed QSNs-WLEDs demonstrated an LE enhancement of 15.7% over conventional mixed-type WLEDs due to the less reabsorption loss. Consequently, the newly proposed QSNs-WLEDs showed 20.5 °C lower QDs working temperature under driving current of 200 mA.**

***Index Terms*— Color-rendering index, luminous efficiency (LE), phosphor, quantum dots (QDs), silica coating, white light-emitting diodes (WLEDs).**

I. Introduction

WHITE light-emitting diodes (WLEDs) have been attracting numerous interests due to their extraordinary characteristics over conventional light sources such as high efficiency, low consumption, environmental protection, and long lifetime [1]–[3]. The most widely used phosphor-converted WLEDs (pc-WLEDs) are realized by combining blue LED chip with yellow-emissive $Y_3Al_5O_{12}$: Ce^{3+} (YAG: Ce) phosphor. The pc-WLEDs can achieve high luminous efficiency (LE), while their color-rendering index (CRI) is relatively low (70) due to the lack of red spectral components [4]. Adding red phosphor is an effective way to remedy the defect of CRI. However, it is incapable of maintaining high LE because the broad red emission partially lies outside the sensitive region of human eyes [5], [6].

Recently, quantum dots (QDs) have attracted extensive attention in solid-state lighting field due to their unique optical properties such as narrow emission spectrum, size-tunable emission wavelength, and high quantum yields [7]. It has been reported that WLEDs composed of blue LED chip, yellow-emissive phosphor, and red-emissive QDs can realize excellent CRI (Ra > 90) as well as remarkably high LE [8], [9], making QDs-WLEDs a potential alternative for the next-generation artificial light source. In the packaging process of QDs-WLEDs, the QDs are impractical for integration of LEDs directly due to their solution-based synthetic route, in which QDs are suspended in some organic solvent. The hydrophobic organic ligands on QDs' surface damage the polymerization of silicone gel, namely, the catalyst-poisoning effect [10]. In addition, the incompatibility of QDs' surface with silicone gel can result in QDs agglomeration, consequently decreasing the photoluminescence (PL) efficiency. Therefore, several solutions have been proposed to solve the compatibility problem, for instance, modifying QDs' surface chemistry [11], [12], incorporating QDs into mesoporous microspheres [13], and coating barrier layer on QDs' surface [14], [15]. Among these approaches, QDs-silica coated nanoparticles (QSNs), e.g., CdSe-SiO_2 [16], CdSe/ZnS-SiO_2 [17], and CdSe/CdS/ZnS-SiO_2 [18], have been widely studied, and the photostability of QSNs/phosphor-silicone mixture has been proven to be dramatically improved after coating. To our knowledge, the existing QSNs-WLEDs are fabricated by directly mixing QSNs with phosphor gel [19]. Because of the strong Mie scattering effect of phosphor particles, yellow photons are partially reabsorbed by QSNs and converted to red photons, resulting in reabsorption energy losses. Moreover, the utilization of QSNs is inefficient because the nanosized QSNs are far away from the LED chip; consequently, increasing the amount of QDs needed.

Manuscript received July 25, 2017; revised November 26, 2017; accepted December 19, 2017. Date of publication December 29, 2017; date of current version January 22, 2018. This work was supported in part by the National Natural Science Foundation of China under Grant 51625601, Grant 51576078, Grant 51376070, and Grant 51402148, in part by Guangdong Innovation Project under Grant 2014A010105005 and Grant 2014TQ01C494, and in part by Tianjin New Materials Science and Technology Major Projects under Grant 16ZXCLGX00040. The review of this paper was arranged by Editor E. G. Johnson. *(Corresponding author: Kai Wang; Xiaobing Luo.)*

B. Xie, Y. Cheng, X. Yu, W. Shu, and X. Luo are with the School of Energy and Power Engineering, Huazhong University of Science and Technology, Wuhan 430074, China (e-mail: luoxb@hust.edu.cn).

J. Hao and K. Wang are with the Department of Electrical and Electronic Engineering, Southern University of Science and Technology, Shenzhen 518055, China (e-mail: wangk@sustc.edu.cn).

Color versions of one or more of the figures in this paper are available online at http://ieeexplore.ieee.org.

Digital Object Identifier 10.1109/TED.2017.2785772

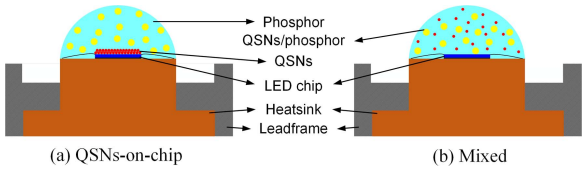

Fig. 1. Schematic shows the (a) separated- and (b) mixed-type QSNs/pc-WLEDs.

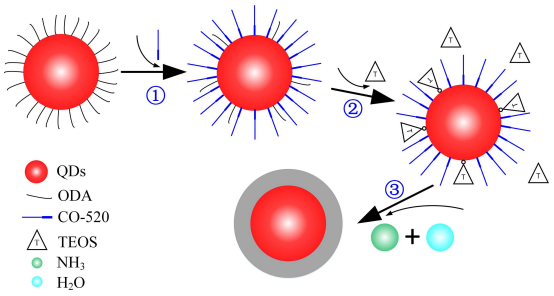

Fig. 2. Schematic showing the synthesis of QSNs by using the microemulsion reaction.

Therefore, in this paper, a silica shell was coated onto the QDs surface to solve the compatibility problem between QDs and phosphor-silicone gel. Then, a QSNs-on-chip packaging structure was proposed to eliminate the reabsorption energy loss. Fig. 1 shows the schematic of the proposed QSNs-on-chip packaging and conventional mixed packaging. Red-emissive CdSe/ZnS core–shell QDs were synthesized, and QSNs were prepared by a microemulsion reaction. For the fabrication of QSNs-on-chip WLEDs packaging, QSNs were directly coated onto the LED chip; then, yellow-emissive YAG:Ce phosphor-silicone gel was coated. The effect of QDs/phosphor reabsorption on the optical energy loss was also discussed. Finally, the temperature fields of the QSNs-on-chip and conventional mixed QSNs-WLEDs were measured to analyze the thermal effect due to the reabsorption energy loss.

II. Experiments

A. Synthesis of Red-Emissive CdSe/ZnS Core/Shell QDs

According to [20], adding QDs with a peak wavelength of 626 nm into phosphor-converted LEDs can greatly improve the CRI. Therefore, high-quality red-emissive CdSe/ZnS core/shell QDs with peak wavelength of 626 nm was prepared by the Tri-n-Octylphosphine (TOP)-assisted successive ionic layer adsorption and reaction (SILAR) method [21].

B. Preparation of CdSe/ZnS-SiO_2 QSNs

To coat the QDs with silica shells, a microemulsion reaction was applied [22]. Fig. 2 shows the synthesis process of QSNs. Briefly, 25 ml of cyclohexane as a solvent and 3 g of IGEPAL CO-520 as a surfactant were mixed at room temperature. A 0.5 mg of QDs dispersed in 0.5 ml of toluene was introduced into the above mixture, and then 0.5 ml (9 m · mol) of tetraethyl orthosilicate was added. The reaction was initiated by adding 0.5 ml of ammonium at the rate of 0.2 ml/min and then it was allowed to proceed for 40 h. After completion of the silica growth, the solution was precipitated by adding methanol and was centrifuged to isolate the QSNs from the microemulsion. The resultant QSNs were washed sequentially with cyclohexane, n-hexane, and finally dispersed in methanol.

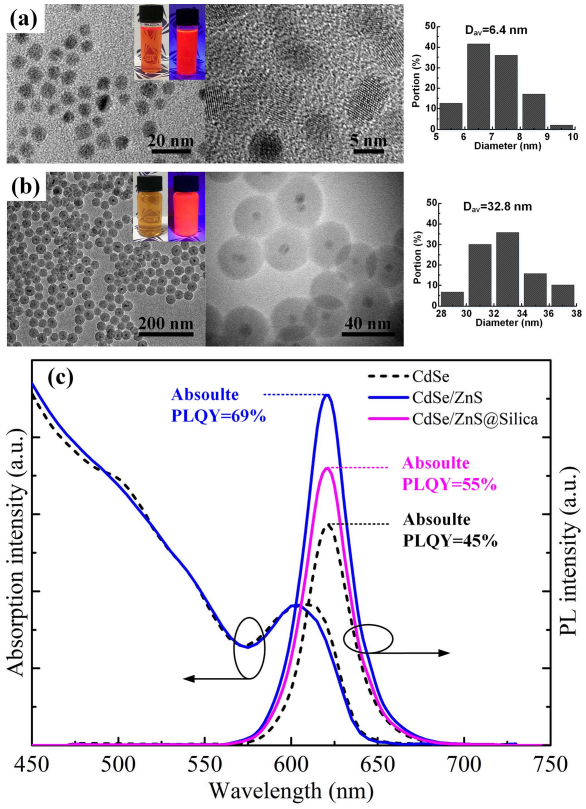

Fig. 3. HRTEM images of the (a) CdSe/ZnS QDs and (b) QSNs. Inset: Corresponding photographs under daylight and UV light. Right graph shows the corresponding diameter distribution. (c) Absorption and PL spectra of the CdSe core QDs, CdSe/ZnS core–shell QDs, and QSNs.

C. Fabrication of QSNs/pc-WLEDs

In the fabrication of separated-type QSNs/pc-WLEDs, QSNs methanol solution was first dripped onto the InGaN LED chip (455 nm), then the module was placed on the hotplate at 70 °C for 10 min. After all the methanol was evaporated, YAG:Ce phosphor (550 nm, Intematix Co.) was mixed homogeneously with silicone gel (Dow Corning OE 6550, A:B = 1:1). Bubbles introduced during the mixing process were removed by applying alternating cycles of vacuum. Then, the phosphor gel was dip coated onto the LED module to cover the LED chip and QSNs. Finally, the phosphor gel was cured by an annealing step at 150 °C for 30 min.

As a comparison, the conventional mixed-type QSNs/pc-WLEDs were also fabricated. First, QSNs methanol solution was mixed homogeneously with phosphor-silicone gel. Then, the methanol solvent was removed by applying 60 °C of heating and vacuum alternately. After all the methanol was evaporated, the resultant was coated onto the LED chip, followed by an annealing step at 150 °C for 30 min.

III. Results and Discussion

Fig. 3 shows the high-resolution transmission electron microscopy (HRTEM) images of the as-prepared CdSe/ZnS

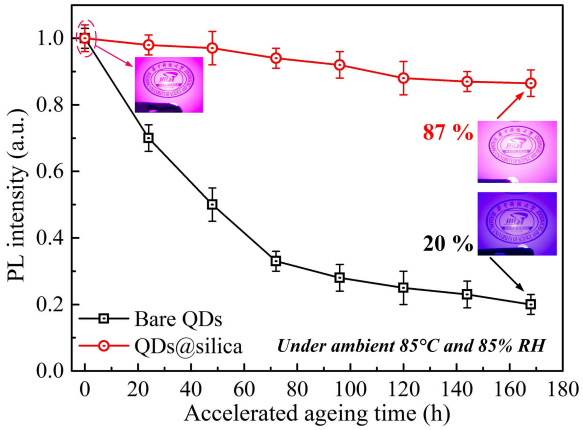

Fig. 4. Normalized decay curves of QSNs and bare QDs-based LED for accelerated aging test. Inset: Corresponding illumination pattern under different aging times.

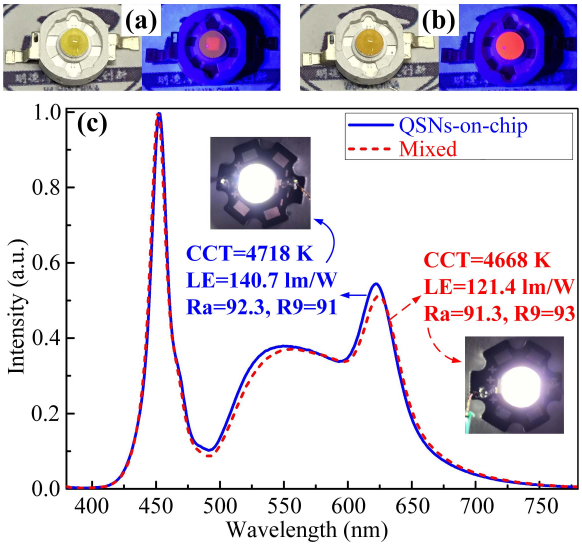

Fig. 5. Photographs of the (a) QSNs-on-chip WLEDs and (b) mixed WLEDs under daylight and UV light illumination. (c) EL spectra of the as-fabricated two types of WLEDs under 20 mA. Inset: Illuminated photographs.

QDs and the QSNs, and the absorption/emission spectra of the core and core/shell QDs. From Fig. 3(a), the QDs' average size is measured as 6.4 nm with uniform size distribution. An advantage from the TOP-assisted SILAR method, which removes the surface lattice imperfections by the surface ions redissolution and lattice rearrangement during the whole ZnS shell formation process, is that the absolute PL quantum yields (PLQY) was efficiently enhanced from 45% (core) to 69% (core–shell), as depicted in Fig. 3(c). Fig. 3(b) shows TEM images of the as-prepared QSNs, which demonstrate good dispersity and uniform size distribution. Under optimized condition, the average particle size is measured as 32.8 nm with silica-coating thickness of about 13.2 nm. This coating thickness can provide effective protection for QDs and retain QDs' PL intensity. The TEM measurements indicate that in the majority of the composite particles, the QDs are located at the center of the structure. Also, only rarely we observe instances of multiple QDs residing within the same silica shell. After silica-coating process, the PL QY of QDs dropped from 69% to 55%. This PL QY attenuation is quite related to the silica-coating thickness. It was also observed that the peak wavelength of QDs after silica coating changes from 629 to 628 nm, which is negligible for the WLEDs packaging process.

An important benefit of silica coating is a significant improvement of long-term photo and thermal stability of the QSNs compared with bare QDs. Therefore, an accelerated aging test was conducted to validate the effectiveness of our silica-shell coating. Three LED samples were fabricated by using the bare QDs and QSNs, respectively. In the fabrication of QSNs-based samples, QSNs methanol solution was first dropped onto the InGaN LED chip, then the module was placed on the hotplate at 70 °C for 10 min. After all the methanol was evaporated, pure silicone gel was coated onto the LED module to cover the LED chip and QSNs, followed by an annealing step at 150 °C for 30 min. Similar procedures were applied in the fabrication of bare QDs-based samples.

In the accelerated aging test, the LED samples were placed into an oven under 85 °C and 85% relative humidity (85 RH) for 168 h. The PL intensity of QDs and QSNs was monitored every 24 h. Fig. 4 shows the accelerated decay curves of these samples. It is seen that at the beginning 48 h, the bare QDs lost 50% of the original PL intensity, while the PL intensity of silica-coated QDs remained intact. After 168-h aging, 87% of the original PL intensity is still preserved for the QSNs, while the bare QDs only retain 20% of the original PL intensity. From the illumination pattern in the insets of Fig. 4, we can clearly observe the degradation of bare QDs sample, which lost most of the red emission at the completion of the 168-h test, while the QSNs samples still show most of the original red emission after the aging test.

Fig. 5 displays the photographs and electroluminescence (EL) spectra of the as-fabricated WLEDs with QSNs-on-chip and mixed packaging structures under 20-mA illumination. These WLEDs were fabricated with identical spectral power distribution. At the same correlated color temperature level of 4700 K (neutral white light), both types reveal high CRI values of Ra > 90, and R9 > 90, which indicates the color-rendering ability toward deep red. It is seen that the proposed QSNs-on-chip type WLEDs achieved an LE of 140.7 lm/W, which is 15.7% higher than that of mixed type (121.4 lm/W). Therefore, benefit from the separated QSNs/phosphor structure, the reabsorption energy loss between QSNs and phosphor can be significantly reduced.

Fig. 6 shows the LE and CRI of these WLEDs under increasing driving current from 20 to 200 mA. Both types of WLEDs show stable spectral distributions without PL saturation effect [23], their CRI values nearly unchanged even at 200 mA (Ra > 88 and R9 > 89). Type I shows enhanced LE than type II under different driving currents, indicating the effective reduction of reabsorption losses. Note that the LE drop with increasing current is mainly attributed to the efficiency drop of LED chip itself.

To further investigate the reabsorption effect, we calculated the optical energy loss of LED chip, QSNs plus phosphor in QSNs-on-chip type, and the mixture of QSNs/phosphor

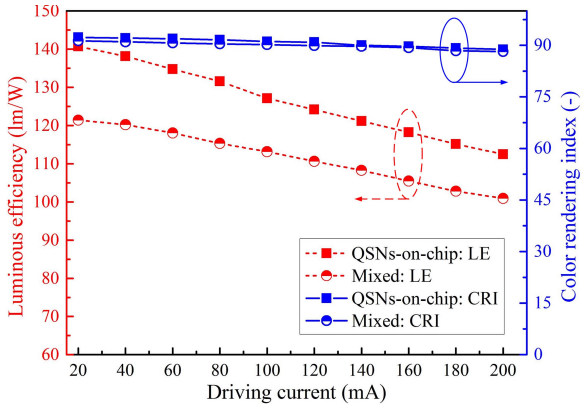

Fig. 6. LE and CRI of the QSNs-on-chip and mixed-type WLEDs under different driving currents.

in mixed type. The energy losses are obtained by calculating the optical energy difference during the packaging process [24], [25]. Also, these reabsorption energy loss can be calculated theoretically [26], [27]. Briefly, the energy loss of "LED chip" is calculated by the difference of input electrical power and output optical power of LED module with only silicone gel; the energy loss of "QSNs plus phosphor" is calculated by the difference of output optical power of LED module with only silicone gel and output optical power of LED module with QSNs plus phosphor gel; the energy loss of "mixture of QSNs/phosphor" is calculated by the difference of output optical power of LED module with only silicone gel and output optical power of LED module with mixed QSNs/phosphor gel.

Fig. 7(a) shows the measured energy loss in each component. The reabsorption energy loss was calculated as 3 mW at 20 mA, 11.4 mW at 100 mA, and 17.1 mW at 200 mA, respectively. Therefore, the reabsorption energy loss increased with the increasing driving current, indicating that the proposed separated packaging structure reduces more energy loss at higher driving current.

Another main concern is that the working temperature of QSNs-on-chip type should be reduced compared to that of mixed type due to the less heat generation. Therefore, we measured the steady temperature fields of these two WLEDs by an infrared thermal imager (FLIR SC620). The WLEDs module is mounted onto a metal core printed circuit board for heat dissipation, and then driven by 200 mA. The emissivity of silicone gel is set as 0.96 [28], [29], and distance between camera lens and WLEDs is set as 0.5 m. Fig. 7(b) displays the measured temperature fields of these WLEDs. It is seen that under the same driving current of 200 mA, the temperature of top silicone in the QSNs-on-chip type is 20.5 °C lower than that in the mixed type.

While, this observed temperature reduction at the top of silicone is insufficient to demonstrate the advantage of our QSNs-on-chip type WLEDs since the highest working temperature was not revealed. Therefore, we simulated the temperature distribution of type II WLEDs by the finite-element method to investigate the location of highest working temperature. Due to the difficulties in measuring the thermal

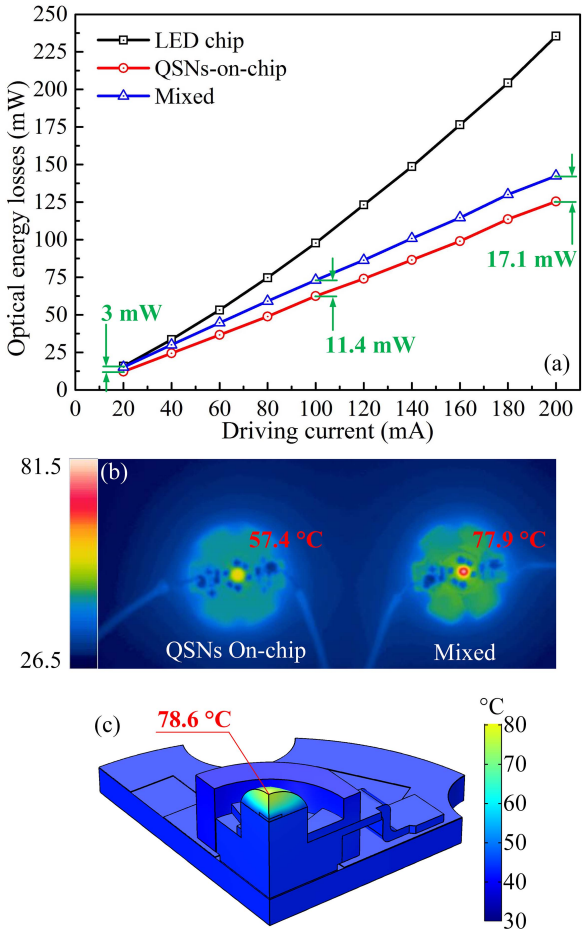

Fig. 7. (a) Optical energy losses of LED chip, QSNs plus phosphor in the QSNs-on-chip type, and QSNs/phosphor mixture in the mixed type. (b) Measured temperature fields of the QSNs-on-chip type and mixed-type WLEDs under driving current of 200 mA. (c) Simulated temperature fields of the mixed-type WLEDs under driving current of 200 mA.

conductivity of QSNs particles, the thermal simulation of type I WLEDs was not conducted in this paper. In the simulation, all the boundary conditions and thermal conductivity settings were the same as those in [30].

Fig. 7(c) shows the simulated temperature field of mixed-type WLEDs under 200 mA. It is seen that the simulated result agrees well with the experiment, and the relative deviation of the highest temperature is less than 1%. The highest temperature of type II WLEDs locates on the top surface of silicone. This is mainly attributed to the relatively low-thermal conductivity of silicone and ambient air. It can be indicated from the simulation result that the highest temperature of QSNs-on-chip type also locates on the top surface of silicone, and its highest temperature is lower than that of mixed type due to the better heat dissipation condition of QSNs. Thus, it is confirmed by both experiments and simulation that the QSNs-on-chip type takes greater advantages over conventional mixed type in both optical and thermal performances.

IV. Conclusion

In this paper, a QSNs-on-chip type WLEDs packaging was proposed to reduce the reabsorption energy loss and

enhance the LE. Highly luminescent red-emissive CdSe/ZnS QDs were synthesized by the TOP-assisted SILAR method. Then, QDs were coated with a silica shell by the microemulsion reaction; subsequently, the QSNs with uniform size distribution and good dispersity were prepared. The QSNs-on-chip type WLEDs were fabricated by first dipping QSNs onto the LED chip, then coating the phosphor-silicone gel. The as-prepared QSNs exhibited excellent luminescent stability over bare QDs under 85 °C and 85% RH. With CRI > 90 and R9 > 90, the newly proposed QSNs-WLEDs demonstrated an LE enhancement of 15.7% over conventional mixed-type WLEDs due to the less reabsorption loss. Consequently, the newly proposed WLEDs showed 20.5 °C lower QDs working temperature under driving current of 200 mA, which is beneficial for QDs' long-term operation.

References

[1] S. Pimputkar, J. S. Speck, S. P. DenBaars, and S. Nakamura, "Prospects for LED lighting," *Nature Photon.*, vol. 3, no. 4, pp. 180–182, 2009, doi: 10.1038/nphoton.2009.32.

[2] X. Luo, R. Hu, S. Liu, and K. Wang, "Heat and fluid flow in high-power LED packaging and applications," *Prog. Energy Combustion Sci.*, vol. 56, pp. 1–32, Sep. 2016, doi: 10.1016/j.pecs.2016.05.003.

[3] H. S. Jang and D. Y. Jeon, "White light emission from blue and near ultraviolet light-emitting diodes precoated with a Sr^3SiO^5:Ce3+, Li^+ phosphor," *Opt. Lett.*, vol. 32, no. 23, pp. 3444–3446, Dec. 2007, doi: 10.1364/OL.32.003444.

[4] H. S. Jang, W. B. Im, D. C. Lee, D. Y. Jeon, and S. S. Kim, "Enhancement of red spectral emission intensity of $Y_3Al_5O_{12}:Ce^{3+}$ phosphor via Pr co-doping and Tb substitution for the application to white LEDs," *J. Luminescence*, vol. 126, no. 2, pp. 371–377, Oct. 2007, doi: 10.1016/j.jlumin.2006.08.093.

[5] X. Piao, K. Machida, T. Horikawa, H. Hanzawa, Y. Shimomura, and N. Kijima, "Preparation of $CaAlSiN_3:Eu^{2+}$ phosphors by the self-propagating high-temperature synthesis and their luminescent properties," *Chem. Mater.*, vol. 19, no. 18, pp. 4592–4599, Sep. 2007, doi: 10.1021/cm070623c.

[6] K. Uheda, N. Hirosaki, and H. Yamamoto, "Host lattice materials in the system Ca_3N_2–AlN–Si_3N_4 for white light emitting diode," *Phys. Status Solidi A*, vol. 203, no. 11, pp. 2712–2717, Sep. 2006, doi: 10.1002/pssa.200669576.

[7] K.-S. Cho *et al.*, "High-performance crosslinked colloidal quantum-dot light-emitting diodes," *Nature Photon.*, vol. 3, no. 6, pp. 341–345, Jun. 2009, doi: 10.1038/NPHOTON.2009.92.

[8] B. Xie, R. Hu, and X. Luo, "Quantum dots-converted light-emitting diodes packaging for lighting and display: Status and perspectives," *J. Electron. Packag.*, vol. 138, no. 2, p. 020803, Jun. 2016, doi: 10.1115/1.4033143.

[9] W. Chen *et al.*, "High efficiency and color rendering quantum dots white light emitting diodes optimized by luminescent microspheres incorporating," *Nanophotonics*, vol. 5, no. 4, pp. 565–572, Sep. 2016, doi: 10.1515/nanoph-2016-0037.

[10] H. Kim *et al.*, "*In situ* synthesis of thiol-capped $CuInS_2$-ZnS quantum dots embedded in silica powder by sequential ligand-exchange and silanization," *Electronchem. Solid-State Lett.*, vol. 15, no. 2, pp. K16–K18, Dec. 2011, doi: 10.1149/2.011202esl.

[11] M. Tamborra, M. Striccoli, R. Comparelli, M. L. Curri, A. Petrella, and A. Agostiano, "Optical properties of hybrid composites based on highly luminescent CdS nanocrystals in polymer," *Nanotechnology*, vol. 15, no. 4, pp. S240–S244, Apr. 2004, doi: 10.1088/0957-4484/15/4/023.

[12] H. Zhang *et al.*, "From water-soluble CdTe nanocrystals to fluorescent nanocrystal–polymer transparent composites using polymerizable surfactants," *Adv. Mater.*, vol. 15, no. 10, pp. 777–780, May 2003, doi: 10.1002/adma.200304521.

[13] W. Chen *et al.*, "Highly efficient and stable luminescence from microbeans integrated with Cd-free quantum dots for white-light-emitting diodes," *Particle, Particle Syst. Characterization*, vol. 21, no. 10, pp. 922–927, Oct. 2015, doi: 10.1002/ppsc.201500074.

[14] B. Zhao, X. Yao, M. Gao, K. Sun, J. Zhang, and W. Li, "Doped quantum dot silica nanocomposites for white light-emitting diodes ," *Nanoscale*, vol. 7, no. 41, pp. 17231–17236, Aug. 2015, doi: 10.1039/c5nr04839g.

[15] C. Zhou *et al.*, "Synthesis of silica protected photoluminescence QDs and their applications for transparent fluorescent films with enhanced photochemical stability," *Nanotechnology*, vol. 23, no. 42, p. 425601, Oct. 2012, doi: 10.1088/0957-4484/23/42/425601.

[16] S. T. Selvan, T. T. Tan, and J. Y. Ying, "Robust, non-cytotoxic, silica-coated CdSe quantum dots with efficient photoluminescence," *Adv. Mater.*, vol. 17, no. 13, pp. 1620–1625, Jul. 2015, doi: 10.1002/adma.200401960.

[17] T. Zhang *et al.*, "Cellular effect of high doses of silica-coated quantum dot profiled with high throughput gene expression analysis and high content cellomics measurements," *Nano Lett.*, vol. 6, no. 4, pp. 800–808, Apr. 2006, doi: 10.1021/nl0603350.

[18] S. Jun, J. Lee, and E. Jang, "Highly luminescent and photostable quantum dot–silica monolith and its application to light-emitting diodes," *ACS Nano*, vol. 7, no. 2, pp. 1472–1477, Jan. 2013, doi: 10.1021/nn3052428.

[19] H. Yoo, H. S. Jang, K. Lee, and K. Woo, "Quantum dot-layer-encapsulated and phenyl-functionalized silica spheres for highly luminous, colour rendering, and stable white light-emitting diodes," *Nanoscale*, vol. 7, no. 30, pp. 12860–12867, Jun. 2015, doi: 10.1039/c5nr02991k.

[20] B. Xie *et al.*, "Realization of wide circadian variability by quantum dots-luminescent mesoporous silica-based white light-emitting diodes," *Nanotechnology*, vol. 28, no. 42, p. 425204, Oct. 2017, doi: 10.1088/1361-6528/aa82d7.

[21] J.-J. Hao, J. Zhou, and C.-Y. Zhang, "A tri-*n*-octylphosphine-assisted successive ionic layer adsorption and reaction method to synthesize multilayered core–shell CdSe–ZnS quantum dots with extremely high quantum yield," *Chem. Commun.*, vol. 49, no. 56, pp. 6346–6348, May 2013, doi: 10.1039/c3cc43147a.

[22] H. Li, K. Wu, J. Lim, H.-J. Song, and V. I. Klimov, "Doctor-blade deposition of quantum dots onto standard window glass for low-loss large-area luminescent solar concentrators," *Nature Energy*, vol. 1, p. 16157, Oct. 2016, doi: 10.1038/NENERGY.2016.157.

[23] X. Lei, H. Zheng, X. Guo, J. Chu, S. Liu, and P. Liu, "Optical performance enhancement of quantum dot-based light-emitting diodes through an optimized remote structure," *IEEE T. Electron Dev.*, vol. 63, no. 2, pp. 691–697, Feb. 2016, doi: 10.1109/TED.2015.2508026.

[24] B. Xie *et al.*, "Structural optimization for remote white light-emitting diodes with quantum dots and phosphor: Packaging sequence matters," *Opt. Exp.*, vol. 24, no. 26, pp. A1560–A1570, Dec. 2016, doi: 10.1364/OE.24.0A1560.

[25] Y. Ma, R. Hu, X. Yu, W. Shu, and X. Luo, "A modified bidirectional thermal resistance model for junction and phosphor temperature estimation in phosphor-converted light-emitting diodes," *Int. J. Heat Mass Transfer*, vol. 106, pp. 1–6, Mar. 2017, doi: 10.1016/j.ijheatmasstransfer.2016.10.058.

[26] J. Li, Y. Tang, Z. Li, X. Ding, D. Yuan, and B. Yu, "Study on scattering and absorption properties of quantum-dot-converted elements for light-emitting diodes using finite-difference time-domain method," *Materials*, vol. 10, no. 11, p. 1264, Nov. 2017, doi: 10.3390/ma10111264.

[27] B. Fan, X. Guo, Y. Zhang, and J. Fan, "Analytical model of photon reabsorption in ZnO quantum dots with size and concentration dependent dual-color photoluminescence," *J. Appl. Phys.*, vol. 121, no. 5, p. 054309, Feb. 2017, doi: 10.1063/1.4975465.

[28] L. Orloff, J. De Ris, and G. H. Markstein, "Upward turbulent fire spread and burning of fuel surface," *Symp. (Int.) Combustion*, vol. 15, no. 1, pp. 183–192, 1975, doi: 10.1016/S0082-0784(75)80296-7.

[29] F. Jiang, J. L. de Ris, and M. M. Khan, "Absorption of thermal energy in PMMA by in-depth radiation," *Fire Safety J.*, vol. 44, no. 1, pp. 106–112, Jan. 2009, doi: 10.1016/j.firesaf.2008.04.004.

[30] B. Xie, R. Hu, X. Yu, B. Shang, Y. Ma, and X. Luo, "Effect of packaging method on performance of light-emitting diodes with quantum dot phosphor," *IEEE Photon. Technol. Lett.*, vol. 28, no. 10, pp. 1115–1118, May 15, 2016, doi: 10.1109/LPT.2016.2531794.

Authors' photographs and biographies not available at the time of publication.